



Research Article

A Novel Low Axis Ratio Double-Circularly Polarized Microstrip Antenna

Jin-Ku Liu , Xi-Lai Zhao , Chen-Xin Zhang , and Zan-Yang Wang 

Air Force Engineering University, Xi'an, 710051, China

Correspondence should be addressed to Chen-Xin Zhang; 15353552791@189.cn

Received 19 November 2021; Revised 25 March 2022; Accepted 26 March 2022; Published 13 April 2022

Academic Editor: Trushit Upadhyaya

Copyright © 2022 Jin-Ku Liu et al. This is an open access article distributed under the Creative Commons Attribution License, which permits unrestricted use, distribution, and reproduction in any medium, provided the original work is properly cited.

This article presents a dual circular polarization (CP) microstrip antenna, emitting electromagnetic waves above and below the substrate, which is fed by the double L-probe. Selecting the L-probe feed increases the bandwidth of the antenna, and different probes control the rotation of CP. The antenna could radiate two polarized waves of the same amplitude and vertical through two square radiation patches; meanwhile, adjusting the phase difference between both waves to 90° will produce a CP wave in the far-field. The simulation and measurement results show that the antenna is in 4.3–4.8 GHz band with $S_{11} < -10$ dB, $S_{22} < -10$ dB, and $AR < 3$ dB. Furthermore, a lower axis ratio could be obtained in this work compared with similar antennas of the same type.

1. Introduction

The circular polarization (CP) microstrip antenna has been widely used in satellite communications due to its strong ability of antidamping, antimultipath interference, and antimultipath reflection [1–6]. The performance of the CP antenna plays a decisive role in a communication system. The generating principle of CP radiation is that the antenna generates two linearly polarized waves with 90° phase difference, mutually orthogonal and equal amplitude. At present, the most widely used approaches to generate CP electromagnetic waves are a multivariate method, many feed method, and single feed method [7].

A dual-sense CP microstrip antenna is proposed in [8]. With the rectangular microstrip antenna operating in TM_{01} mode as the foundation, a single-coupled line is adopted to excite the TM_{10} mode with a phase difference of 90° , which leads the generation of a CP operation. Different polarization modes can be obtained by changing the position of the single coupling line; therefore, double coupled lines can be employed in the rectangular microstrip antenna to generate two CP radiations. However, the axial ratio of this antenna is narrow. Reference [9] presents a low-cost single layer dual CP series-fed antenna based on the sequential rotation technique. The antenna is made of curved microstrip lines as

radiation elements of the antenna, which can be directly printed on a single layer of PCB without complicated processing and assembly. Therefore, the cost of the antenna is low and suitable for mass production, but the axial ratio bandwidth of the antenna is only about 10%. Right-handed and left-handed CP can be achieved in the same frequency band by using circular grooves and two orthogonal L-shaped feeders in the ground plane. At the same time, the CP performance of the antenna can be improved by properly cutting slots and adding parasitic elements on the ground plane. Though the proposed antenna has a larger axial ratio, its gain becomes lower [10]. Moreover, all the antennas above use one surface radiation; this causes the other patches to gain unwanted coupling, resulting a great impact on the axis ratio. When the patches above and below the substrate radiate simultaneously, the coupling of the electric field can be reduced, getting a lower axial ratio. Meanwhile, the probe feed will be selected to obtain a larger gain.

There are many ways to generate resonance. Reference [11] is able to achieve dual-frequency by mixing slot and patch. In [12], another resonance is generated by introducing a 2×2 SRR array in the ground plane. The multiple resonances in [13] are formed by the alternate use of circular and rectangular slots. The open-loop resonator will produce two different resonances [14]. Finally, we choose the L-probe

as the feed to obtain resonance because it will obtain greater gain.

In this article, an antenna radiating from patches on both surfaces of a substrate is proposed. Two rectangular microstrip patches that are perpendicular to each other can provide two linearly polarized waves of the same frequency and amplitude. Considering it can transmit electricity through metal columns and patches, the phase difference can be adjusted to 90° by adjusting the length of the patch. This antenna degeneracy mode is the same as the microstrip line because the antenna is fed by the probe, and the substrate thickness is much smaller than the operating wavelength. Finally, its axial ratio bandwidth can reach 12%. Furthermore, its axial ratio is less than 3 dB in 4.3 GHz to 4.8 GHz, and its left and right polarization gain can reach more than 5 dB. Compared with the single-sided radiation antenna, this work can effectively reduce the axial ratio, which is especially suitable for satellite communication.

2. Antenna Design

2.1. Element Design. Theoretically, most microstrip antennas radiate from only one surface of the substrate. When feed is applied to the probe, the coupling of the other patches is triggered, generating some undesired currents and leading to higher axial ratios. To reduce unnecessary coupling, two radiation patches were placed on the upper and lower surface of the substrate. To further reduce the coupling, the substrate should be thick enough, and a 2 mm thick substrate shall be selected.

To obtain higher bandwidth, the antenna is fed by an L-shaped probe and the length of the probe should be $\lambda/2$. The radiation patch should choose square patches to obtain greater coupling and higher gain. In order to achieve better resonance of the antenna, the side length of the radiation patch of the antenna should be $\lambda/4$. To make the phase difference between two lines polarization to be 90° , the length of the connecting microstrip line should also be $\lambda/4$. Finally, a metal column is used to connect the radiation patches on the upper and lower surface of the substrate.

Figure 1 shows the structure of the antenna; the antenna size of the antenna is $0.87 \lambda \times 0.87 \lambda \times 0.23 \lambda$ (52 mm \times 52 mm \times 14 mm). It is printed on Teflon glass cloth plate (F4BM-2) substrate ($\epsilon_r = 2.2$; $\tan \theta = 0.001$).

The antenna radiation patch consists of two square copper pieces on the top and bottom that receive the energy from the L-shaped probe in a coupled manner, while two different probes control two directions of rotation of circular polarization. When port 1 is fed, the antenna is right-handed polarized; if port 2 is fed, the antenna is left-handed polarized.

Firstly, by adjusting the probe length, the resonant frequency can reach 4.5 GHz. Then, the side length of the rectangular radiating plate is adjusted to minimize the return loss. Finally, the length of the microstrip line is adjusted so that the antenna axial ratio is less than 3 dB. However, due to the different distance between the patch and the floor, in order to ensure that the resonant center frequency is 4.5 GHz, it is important to ensure that the patch length on

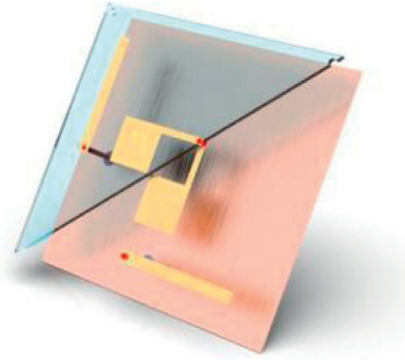


FIGURE 1: Configurations of the antenna.

the top and bottom surfaces of the substrate is different, and the bottom patch must be slightly longer.

The antenna is designed to operate in the C-band, which is currently the most commonly used satellite service. The geometrical parameters indicated by Figure 2 are shown in Table 1; meanwhile, the geometrical parameters are optimized using the ANSYS HFSS 15 simulator.

To better simulate the antenna, we should learn about the boundary conditions and far-field conditions. The boundary condition of the antenna is that the distance between the radiation boundary and the radiator is greater than $1/4 \lambda$. Since the center frequency is 4.5 GHz, the distance should be greater than 16.5 mm, and the specific distance is 20 mm for convenience. The far-field condition of the antenna is that the measured distance is greater than $2D \times D/\lambda$, where D represents the maximum size of the antenna and λ represents the wavelength of the antenna. Therefore, the far-field condition of the designed antenna in this article is greater than 162 mm.

2.2. Working Principle of CP Radiation. The generation of the double CP antenna can be analyzed by the surface current of the antenna [8, 15]. Figure 3 simulates the current distribution on the antenna at 4.5 GHz. Figure 3(a) shows the distribution of the overlapping currents at the port 1 feed. The top patch of the medium radiates current in the $-X$ direction and the bottom patch radiates current in the $-Y$ direction. Because the current is transmitted through the patch, a phase difference of 90° is generated between the two linear polarizations, resulting in a right-handed polarization wave. Figure 3(b) shows the overlapping current distribution at the port 2 feed. The upper patch radiates current in the $+X$ direction and the lower patch radiates current in the $+Y$ direction. There is also a 90° phase difference between the two linear polarizations, which leads to a left-handed polarization wave. Through the analysis and calculation of electric field and magnetic field, TM₁₀ mode is the resonant mode of the antenna.

3. Results and Discussion

3.1. Radiation Pattern and Gain. Figure 4(a) shows the simulation S-parameters of the antenna; the results show that the antenna has an impedance bandwidth of -10 dB

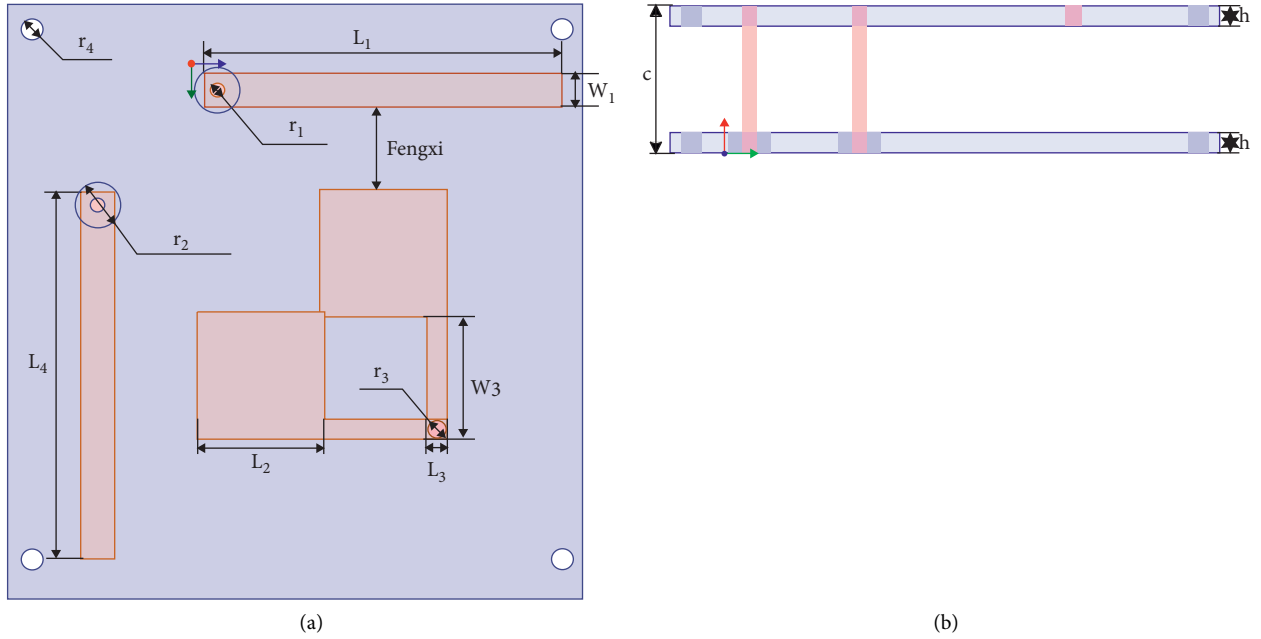


FIGURE 2: Antenna size diagram (all dimensions are indicated in the drawing). (a) Top view. (b) Side view.

TABLE 1: Dimension of the CP antenna (all dimensions are in mm).

L_1	L_2	L_2	L_4	W_1	W_3	r_1
32.4	11.5	1.8	33.2	3	11.1	1.3
r_2	r_3	r_4	C	h	h_1	FENGXI
4.1	1.6	2	14	2	2	7

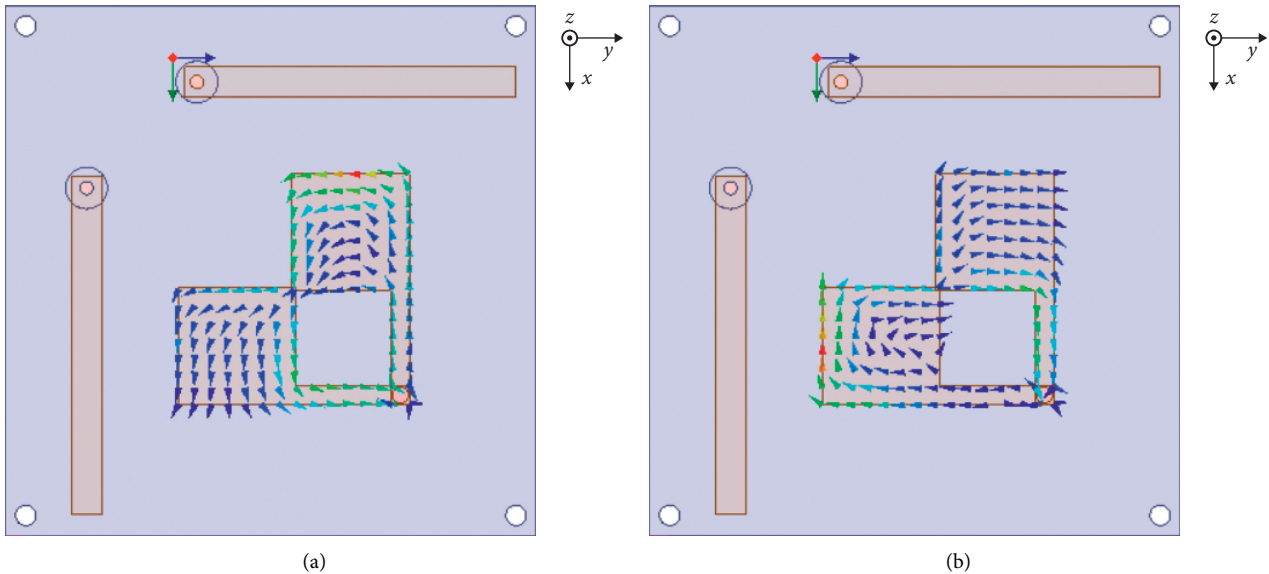


FIGURE 3: Current direction diagram: (a) port 1 and (b) port 2.

ranging from 4.2 GHz to 4.8 GHz when port 1 is working, corresponding to a 13.3% fractional bandwidth. When port 2 is operating, the antenna's -10 dB impedance bandwidth is between 4.2 GHz and 4.88 GHz, corresponding to a 15% fractional bandwidth.

Figure 4(b) shows the axial ratio along $+Z$ direction; moreover, the axial ratio is less than 3 dB within the impedance bandwidth. When port 1 is working, the axial ratio in the range of 4.3 GHz to 4.65 GHz is less than 2 dB. When port 2 is working, the axial ratio in the range of 4.4 GHz to

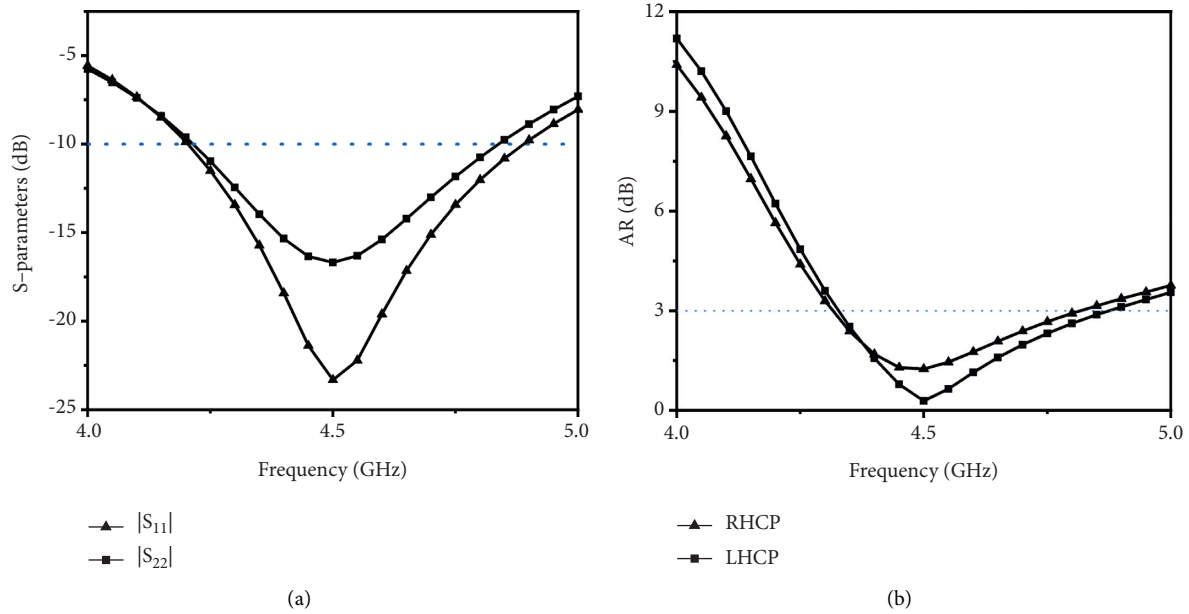


FIGURE 4: The simulation results. (a) Simulated S-parameters. (b) AR.

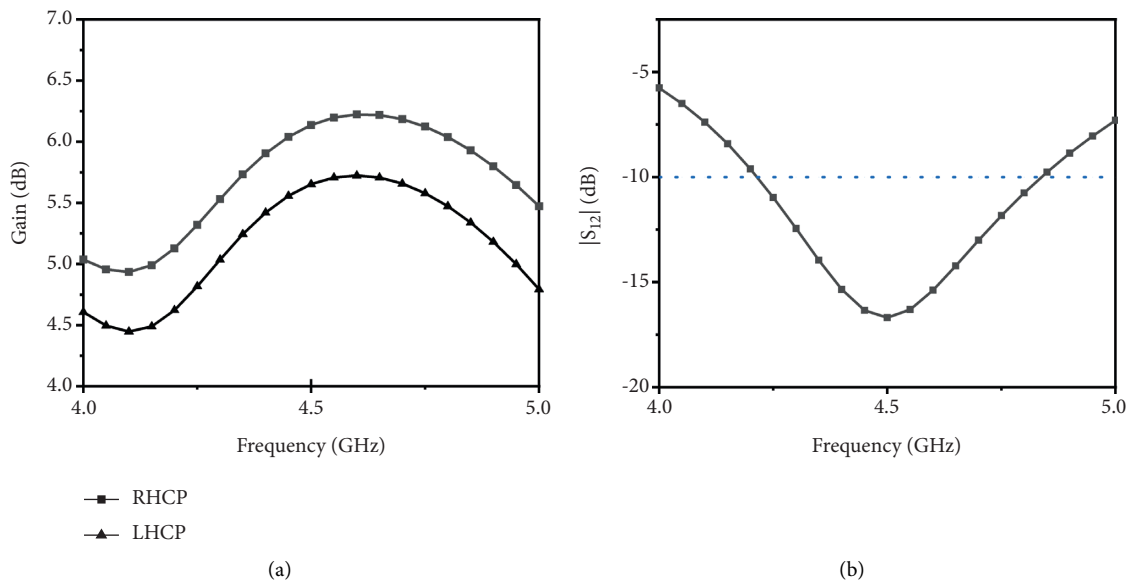


FIGURE 5: The simulation results. (a) Gain. (b) S_{12} .

4.7 GHz is less than 2 dB, accounting for more than 60% of the impedance bandwidth.

Figure 5(a) shows a peak gain of 6.2 dB for right-handed polarization and 5.7 dB for left-handed polarization at 4.6 GHz. Within the bandwidth, both gains are greater than 5 dB, which is within the typical gain range of microstrip antennas. Figure 5(b) shows that S_{12} in the bandwidth is less than -10 dB.

It can be seen that the structure has the advantage of low axis, but it also has a disadvantage that is difficult to overcome. Because the thickness of the dielectric substrate is 2 mm, the height between the antenna and the ground cannot be neglected. Therefore, to make the antenna

resonate at the same frequency, only the lengths of the upper and lower patches need to be adjusted. However, if the axial ratio of one port is changed separately, the axial ratio of the other port will also change. Therefore, it is difficult to match the axial ratio with the return loss, and the probe can only be adjusted so that the two axial ratios overlap as much as possible.

3.2. Measurements and Performance Comparison. Figure 6 shows the simulation and measurement results, and the manufacturing of the antenna is shown in Figure 7. Notable, it is a little bit different between the measured curve

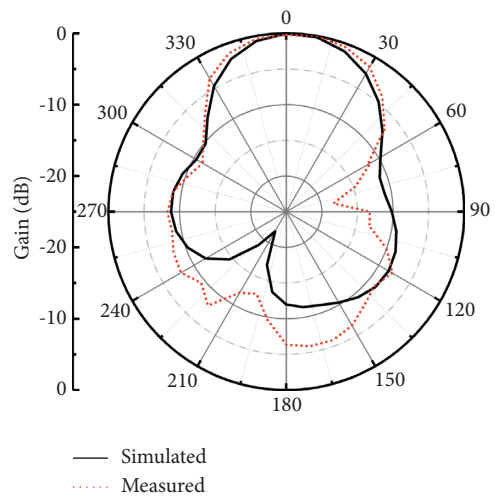
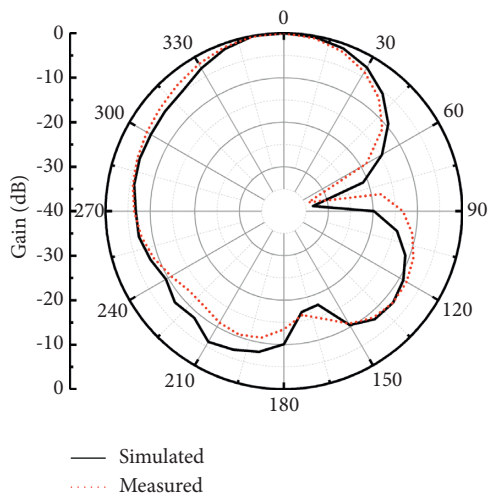
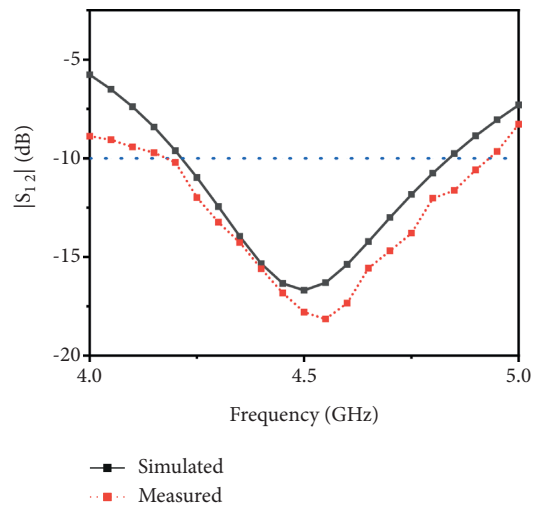
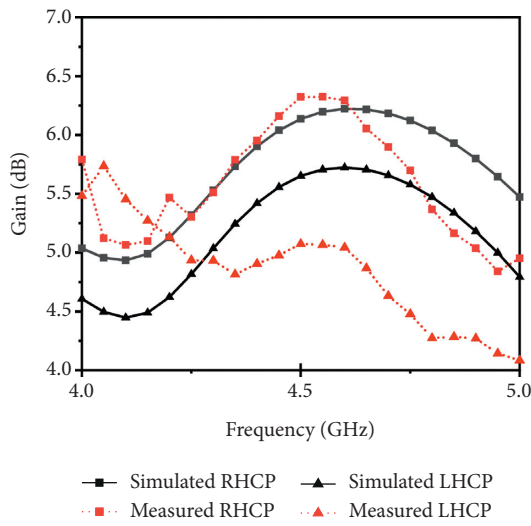
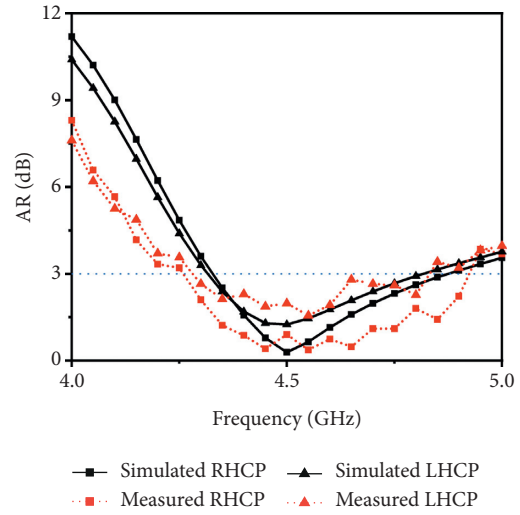
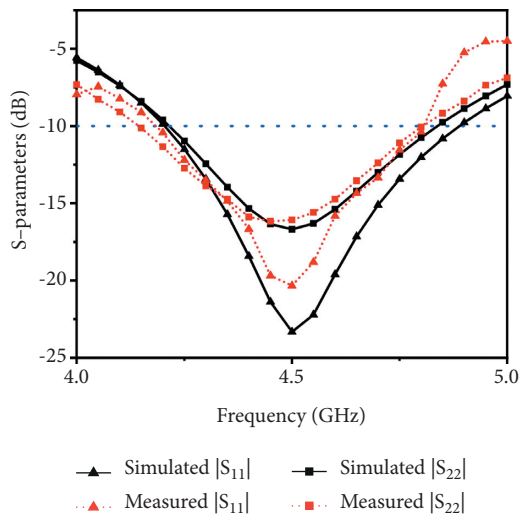


FIGURE 6: Continued.

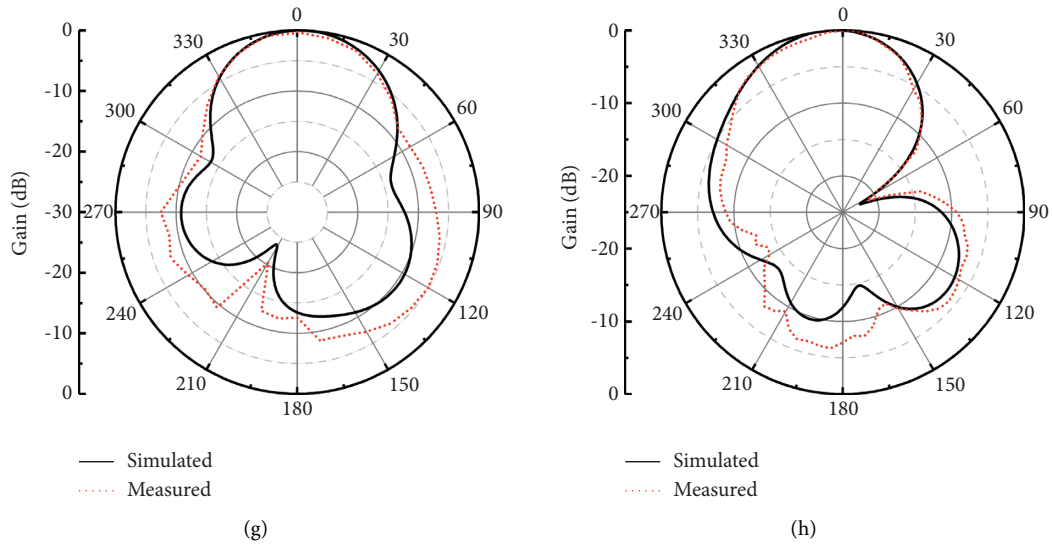


FIGURE 6: Comparison between simulation and measurement. (a) S-parameters, (b) AR, (c) gain, and (d) S12. At 4.5 GHz, dextrally polarized radiation is normalized in the (e) XOZ and YOZ (f) planes and left-handed polarized radiation is normalized in the (g) XOZ and (h) YOZ planes.

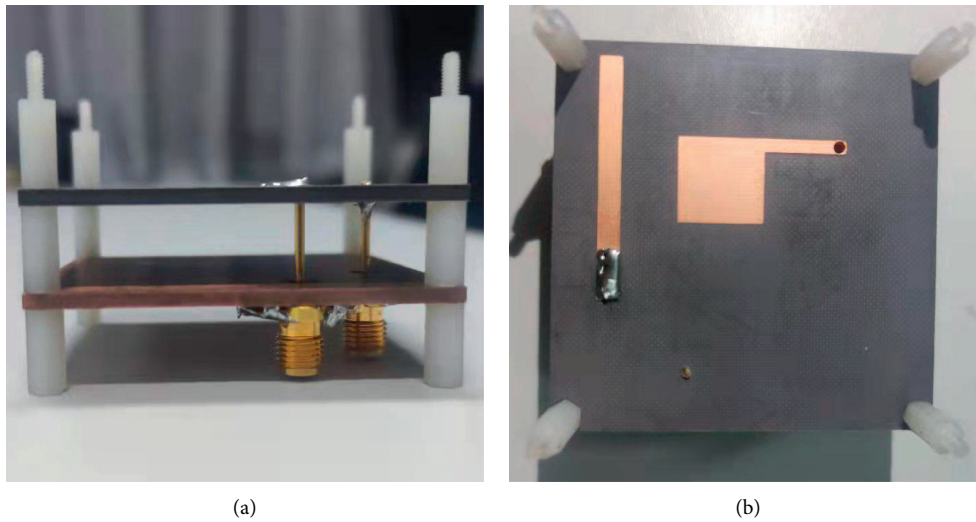


FIGURE 7: Under the close shot, the CP antenna picture of real products. (a) Side view. (b) Top view.

TABLE 2: Comparison of CP antennas.

Ref.	f_0 (GHz)	$ s_{11} B$ (%)	AR BW (%)	Size	Gain (dBi)	P
[8]	2.390	7.95	0.33	$0.44 \times 0.48 \times 0.024$	5.3	LHCP
	2.475		0.72	$0.28 \times 0.39 \times 0.024$	5.7	RHCP
[9]	30	6.75	8.00	$3.5 \times 2.8 \times 0.051$	11.81	Dual
[10]	3.99	59	40.5	$0.63 \times 0.63 \times 0.016$	3.27	Dual
Proposed	4.5	13.7	12.0	$0.77 \times 0.77 \times 0.208$	5.7	LHCP
		15.0	11.0		6.2	RHCP

and the simulation curve. Due to the antenna's fabrication, welding and measurement being different from the ideal situation, there is a certain deviation in the gain and

S-parameters. As shown in Table 2, in terms of axis ratio, its axis is smaller than [8, 9]. Although the axis of [10] is larger, the gain of the antenna is lower.

4. Conclusion

In this article, a new type of dual circularly polarized antenna is proposed, which adopts a new structure of double-sided electromagnetic radiation and effectively reduces the axis ratio. The antenna was simulated, fabricated, and tested, and the results are as expected. This verifies the feasibility of the double-sided radiating electromagnetic wave antenna. Consider the antenna has an advantageously of low axial ratio, it can become a good candidate for satellite communication.

Data Availability

The data used to support the findings of this study are included within the article.

Conflicts of Interest

The authors declare that they have no conflicts of interest.

Authors' Contributions

Jin-Ku Liu and Xi-Lai Zhao contributed equally to this work

Acknowledgments

This study was supported by Natural Science Foundation of Shaanxi Province under Grant: 2016JQ6001.

References

- [1] Q.-S. Wu, X. Zhang, and L. Zhu, "A feeding technique for wideband CP patch antenna based on 90° phase difference between tapped line and Parallel coupled line," *IEEE Antennas and Wireless Propagation Letters*, vol. 18, no. 7, pp. 1468–1471, 2019.
- [2] S.-K. Lin and Y.-C. Lin, "A compact Outer-fed Leaky-wave antenna using Exponentially tapered slots for Broadside circularly polarized radiation," *IEEE Transactions on Antennas and Propagation*, vol. 60, no. 6, pp. 2654–2661, 2012.
- [3] I.-C. Deng, J.-B. Chen, Q.-X. Ke, J.-R. Chang, W.-F. Chang, and Y.-T. King, "A circular CPW-FED slot antenna for broadband circularly polarized radiation," *Microwave and Optical Technology Letters*, vol. 49, no. 11, pp. 2728–2733, 2007.
- [4] Y. W. Liu and P. Hsu, "Broadband circularly polarised square slot antenna fed by coplanar waveguide," *Electronics Letters*, vol. 49, no. 16, pp. 976–977, 2013.
- [5] A. K. Gautam and B. Kr Kanaujia, "A novel dual-band asymmetric slit with defected ground structure microstrip antenna for Circular Polarization operation," *Microwave and Optical Technology Letters*, vol. 55, no. 6, pp. 1198–1201, 2013.
- [6] F. F. Dubrovka and S. Y. Martynyuk, "Wideband dual polarized planar antenna arrays," in *Proceedings of the International Conference on Antenna Theory and Techniques (ICATT)*, pp. 91–96, IEEE, Sevastopol, Ukraine, 9–12 Sept. 2003.
- [7] G. D. Han, K. Chen, and J. D. Yuan, "Small circularly polarized microstrip antenna applied to Beidou navigation terminal," *Modern Radar*, vol. 39, no. 12, pp. 64–66, 2017.
- [8] Z. Zhao, F. Liu, J. Ren, Y. Liu, and Y. Yin, "Dual-sense circularly polarized antenna with A coupled line," *IEEE Antennas and Wireless Propagation Letters*, vol. 19, no. 8, pp. 1415–1419, 2020.
- [9] Y.-H. Yang, B.-H. Sun, and J.-L. Guo, "A low-cost, single-layer, dual circularly polarized antenna for Millimeter-wave applications," *IEEE Antennas and Wireless Propagation Letters*, vol. 18, no. 4, pp. 651–655, 2019.
- [10] F. Liu, X. Y. Zhao, H. Z. Zhao, and Z. N. Jiang, "A novel double-circularly polarized planar microstrip slot antenna is presented," *Journal of Xidian University*, vol. 47, no. 3, 2020.
- [11] T. Upadhyaya, A. Desai, R. Patel, U. Patel, K. P. Kaur, and K. Pandya, "Compact transparent conductive oxide based dual band antenna for wireless applications [C]," in *Proceedings of the 2017 Progress in Electromagnetics Research Symposium - Fall (PIERS - FALL)*, IEEE, Singapore, 19–22 Nov. 2017.
- [12] U. Patel and T. K. Upadhyaya, "Design and analysis of compact μ -negative material loaded wideband electrically compact antenna for wlan/wimax applications," *Progress In Electromagnetics Research M*, vol. 79, pp. 11–22, 2019.
- [13] U. Patel, M. Parekh, A. Desai, and T. Upadhyaya, "Wide slot tri-band antenna for wireless Local Area Network/World Wide Interoperability for Microwave access applications," *International Journal of Communication Systems*, vol. 34, no. 12, 2021.
- [14] U. Patel and T. K. Upadhyaya, "Dual band planar antenna for GSM and WiMAX applications with inclusion of modified split ring resonator structure," *Progress In Electromagnetics Research Letters*, vol. 91, pp. 1–7, 2020.
- [15] S. Liu, D. Yang, and J. Pan, "A low-Profile broadband dual-circularly-polarized Metasurface antenna," *IEEE Antennas and Wireless Propagation Letters*, vol. 18, no. 7, pp. 1395–1399, 2019.